Desalination and Water Treatment
www.deswater.com

doi:10.5004/dwt.2017.21004

87 (2017) 14–26
August

Seven-effect 2 × 4500 m^3/d low temperature multi-effect desalination plant. Part II: A comparative analysis

Chun-hua Qi, Hong-qing Lv*, Hou-jun Feng, Qing-chun Lv

Institute of Seawater Desalination & Multipurpose Utilization, SOA, No.1, Keyan East Road, Nankai District, Tianjin 300192, China, email: qi_chunhua@163.com (C.-H. Qi), Tel./Fax (+86) 022-87898150, email: lvhongqing10@163.com (H.-Q. Lv), dhsfhj@163.com (H.-J. Feng), qclvopen@126.com (Q.-C. Lv)

Received 3 January 2017; Accepted 31 May 2017

ABSTRACT

The operation parameters and performance comparison analysis of seven-effect 2 × 4500 m^3/d low-temperature desalination system matched with the Indramayu 3 × 330 MW coal-fired power-plant were highlighted in this paper. The mathematical model, parameters and materials of the plant are described in detail. The coupling technologies of multi-effect evaporation, multi-stage flash and steam compression are discussed. The influences of the number of effect evaporator on the system GOR, amount of intake seawater, mass flow rate of motive steam and the specific heat transfer area were investigated. The thermal efficiency of the system is fully improved by using a steam compressor during desalination. The best suction pressure of TVC is obtained through numerical analysis of the effect of suction pressure on GOR and amount of cooling seawater. The testing results under the design condition demonstrated that the gained output ration could be increased to 10.3. The error between the operation performance parameter and model values is less than 5%.The operation performance parameters are better than the model calculation values, thereby confirming the accuracy of the established model. This model can provide a reliable tool for approach and determination method of key technical parameters of large scale MED-TVC device, especially for the research and application of desalination facility in the dual-purpose power plant.

Keywords: Number of effect evaporator; Design calculation model; Thermal efficiency; Energy consumption; Performance analysis

1. Introduction

Desalination is a key component toward a sustainable water supply for the continuously population growth and industrial development, given the vast sources of accessible saline water. More than 18,000 desalination plants have been commissioned globally, providing an online capacity of more than 90 million m^3 of water every day [1]. Various approaches have been implemented to desalinate saline water with different performance characteristics [2]. Currently two conventional desalination methods used in seawater desalination are thermally-driven multi-effect desalination (MED) and pressure-driven reverse osmosis (RO) [3].Thermal desalination processes currently account for more than 65% of the production capacity of the desalination industry [4]. Among the thermal desalination systems, multi-effect distillation and thermal vapor compression (MED-TVC) systems with top brine temperature (TBT) lower than 70°C have received considerable attention [5,6]. In these systems, a steam jet ejector is added to a multi-effect distillation (MED) system to reduce the amount of required steam (motive steam), boiler size, and amount of cooling water, thereby reducing pumping power and pretreatment costs [7]. The system gain output ratio (GOR) is much higher when the thermal vapor compression (TVC) system is used compared with that of standalone MED systems. The modeling and single optimization of MED-TVC systems have been investigated. Bin Amer's [8] approach

*Corresponding author.

was applied to maximize the GOR of a MED-TVC system. El-Dessouky et al. [9] and Zhao et al. [10] developed steady-state mathematical models to represent a MED-TVC desalination system in which parametric techniques were used to determine the optimum operating and design conditions. Meanwhile several technologies have been developed and investigated to improve the thermal efficiency of MED system, such as the coupling of multi-effect distillation and adsorption desalination (MED-AD), absorption heat pump, low grade heat utilization technologies, humidification-dehumidification desalination (HDH) and heat transfer enhancement technology [11–14]. Muhammad Wakil Shahzad et al. proposed a hybrid desalination process in order to break the last stage temperature limitation in Gulfand constructed a MED-AD hybrid pilot, with a nominal water production of 10m^3/d. It has found that the proposed hybrid MED-AD cycle has the lowest water production cost compared to conventional ever reported MED process [15,16].

The previous studies have always been focused on the modeling approach and thermo dynamic analyses of MED-TVC desalination systems. Alasfour et al. [17] and Ettouney [18] performed thermal analysis simulations for MED systems. A.S. Hanafi et al. [19] described a 1-D mathematical modeling and conducted CFD investigation on supersonic steam ejector in an MED-TVC system. Aly and Marwan [20] developed a dynamic model for a multi-effect process which laid the foundation for other dynamic models, such as the six-effect evaporator model built by Kumar et al. [21]. De la Calle [22] described a model to simulate the thermal transient behavior of the first cell of a solar-assisted MED plant. Chunhua [23] designed and analyzed the performance of a 30 t/d low-temperature multi-effect evaporation seawater desalination system based on the mathematical model. Although these studies present the operation characteristics for MED or MED-TVC systems, they do not illustrate how process parameters were selected in the MED system. Especially there are few studies focused on the problem 'how to designate the number of effect evaporators in thermal desalination system according to the design conditions'.

On the other hand, a number of reports about the simulation of MED or MED-TVC (including modeling and heat and mass transfer) and performance analysis of small devices has been published. However, the practical desalination equipment are developed towards large-scale, which can reduce the processing, construction, operation, and management costs of equipment, share communal facilities investment, and reduce labor and maintenance costs. Ultimately, this technology can effectively reduce investment and water-making cost per ton.

This paper focuses on the application of MED plant located in Indramayu, Indonesia. The following sections discuss the elements of the desalination plant, which include design conditions, brief process description, modeling, three-dimensional visual design, installation, especially the relationship between number of effect evaporators and the system performance. The Indramayu 2 × 4500 m^3/d MED desalination device supplies fresh water for power plant domestic water and boiler feed water. This device is an important corollary equipment of the Indramayu 3 × 330 MW coal-fired power station project. The project is one of 10 coal-fired power plant projects of the Indonesian government. The project has a total installed capacity of 10,000 MW and is located in west Java province, approximately 180 km east of Jakarta. The performance test of the MED plant was completed, and the testing results showed that the technical indicators achieved the design requirements.

2. Design parameters and requirements

The technical process design of desalination depends on many factors, such as the required gained output ratio, cost of fuel energy charged to the desalting process, electricity sales, capital costs, and local requirements [24,25]. The device operating conditions and design requirements are described as follows.

2.1. Design conditions

(1) Raw water sources and water quality

Raw water of the desalination equipment was taken from the coastal area of Java Island around the north of the power plant. The suspended solid content of the raw water varies from 100 up to 150 mg/L, and the salinity ranges from 33000 mg/L to 34000 mg/L. The design temperature of raw water are determined to be 30°C. Specific water quality indicators are shown in Table 1.

Seawater quality limitation in the desalination system to reduce corrosion of the heat transfer tubes is shown in Table 2.

(2) Steam

The quality indicators of motive steam was 0.8 MPa at 350°C. The quality of steam for driving the steam-jet pump,

Table 1
Analysis of seawater quality

No.	Parameter	Water analysis	
		Location A	Location B
	Physical		
1	TDS, mg/L	33,415	33,575
2	Temperature,°C	30	30
3	Conductivity, μs/cm	42.3	42.3
	Chemical		
4	pH	7.97	7.90
5	Silt, mm	≤1.0	≤1.0
6	Free chlorine, mg/L	0.67	0.86
7	Petroleum like matters, mg/L	≤1.0	≤1.0
8	COD_{Mn}, mg/L	≤5	≤5
9	H_2S, mg/L	≤0.1	≤0.1
10	Free oil, mg/L	≤1.0	≤1.0

Location A: 2 km away from the coastal of Java Island north of the power plant
Location B: near the coast of Java Island north of the plant.

which forms the vacuum condition of the desalination system, was similar to motive steam.

2.2. Device design requirements

The capacity of water produced by the single device was not less than 4500 m^3/d, not including the first-effect production, under the following operating conditions: steam, 0.8 MPa; operating temperature, 350°C; original water temperature, 30°C and salinity, from 33000 mg/L to 34000 mg/L. The total dissolved solid of freshwater was not less than 10 mg/L. GOR was not less than 10. The amount of steam consumed in the GOR calculation refers only to the motive steam, that is, the amount of steam consumed by the vacuum pump was not considered.

Table 2
Seawater quality requirements

Symbol	Value
Suspended solids, mg/L	≤20
pH	6.8~8.8
Silt, mm	≤1
Cl^-, mg/L	0.5~1.0
Petroleum like matters, mg/L	≤1.0
COD_{Mn}, mg/L	≤8
TDS, mg/L	≤50000
H_2S, mg/L	0.1
Free oil, mg/L	1

3. System modeling

The single-effect evaporation process is the technological base of multi-effect desalination regardless of the flashing process. The mathematical model of a single-effect distillation system includes mass balance, energy conservation in the evaporator and condenser, boiling point rise, and thermal loss [26]. These parameters reflect the laws of single-effect evaporation. Modeling approach and process of the shell-and-tube falling film evaporator are the most basic elements for a multi-effect distillation process. El-Dessouky et al. discussed the modeling approach of parallel feed and forward feed, and evaluated systematically the performance of the multiple effect evaporation systems combined with various types of heat pumps [27]. Bourouni and Martin [28] developed a model for heat-and-mass transfers in an air-water-vapor mixture desalination plant, thereby resulting in a set of classical equations. The model can well predict the trends of the heat and mass characteristics of the evaporator. The mathematical model of the 2 × 4500 m^3/d desalination system was established according to the design requirements and multi-effect evaporation specific technological process.

3.1. Model description

The technological process of the MED plant is illustrated in Fig. 1. As shown, the system includes n effect evaporators and n – 1 flashing boxes. Each effect evaporator includes vapor space, demister, condenser/evaporator tubes, brine spray nozzles, and brine pool. In the system, the effect evaporators are numbered 1 to n from the left to right (the direction of the heat flow). Vapor flows from

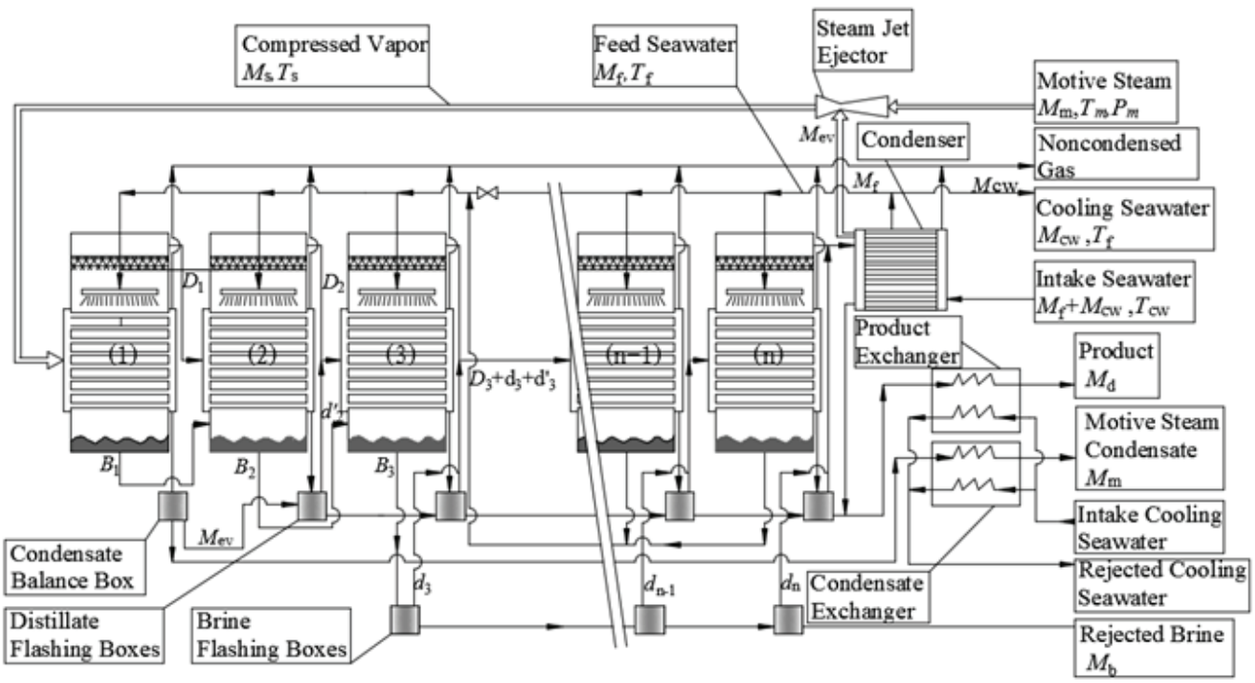

Fig. 1. MED-TVC process model.

left to right, in the direction of pressure drop, and the feed seawater flows in a perpendicular direction. Compressed vapor is introduced into the tube side in the first effect; while, on the shell side, feed seawater is sprayed on the top rows of the tubes. The brine spray forms a thin falling film on the succeeding rows within the evaporator. In the first effect, the brine falling film absorbs the latent heat of the compressed vapor (as shown in Fig. 2). As a result, the brine temperature increases to saturation, where, evaporation commences and a smaller amount of vapor forms. This vapor is used to heat the second effect, where, it condenses on the tube side and releases its latent heat to the brine falling film. This process is repeated for all effects, until effect *n*.

The vapor formed in the last effect evaporator is imported into the condenser. A controlled amount of intake seawater is routed into the tube side of the condenser, where it condenses part of the vapor formed in the last effect. The steam jet ejector entrains the remaining part of the vapor, where it is compressed by the motive steam to the desired pressure and temperature. The warm intake seawater stream leaving the condenser is divided into two parts; the first is the feed seawater stream, which is sprayed distribution among the effect evaporators, and the second is the cooling seawater stream, which is rejected back to the sea. The cooling seawater stream removes the heat added to the system by the motive steam.

The condensate from the first effect evaporator enters into the condensate balance box, and it is delivered separately to the chemical system provided inside the power plant via the condensate heat exchanger, not mixing with the condensate from other effects. The condensed vapor in effects from 2 to *n* is introduced into the associated flashing box, where the temperature of the condensed vapor is reduced through flashing of a small amount of vapor. The flashed off vapor is routed into the tube side of the next effect together with the vapor formed by evaporation or flashing within the previous effect. All the product water is collected and delivered to the product heat exchanger, where the product water is cooled by intake cooling seawater. The brine leaving the first effect is introduced into the brine pool of effect 2. As a result of the positive temperature difference of the brine in effect 1 and 2, a small portion of the feed brine flashes off as it is introduced into effect 2. The flashed off vapors improves the system productivity and thermal efficiency. This process is repeated until effect 3. The remaining concentrated brine from effect 3 enters into the brine flashing boxes to repeat the above process because of temperature difference until effect *n*. Then, the concentrated brine goes through the system in turn. Finally the brine is collected and delivered to the brine heat exchanger in which recovery heat from brine, then directly rejected to the sea.

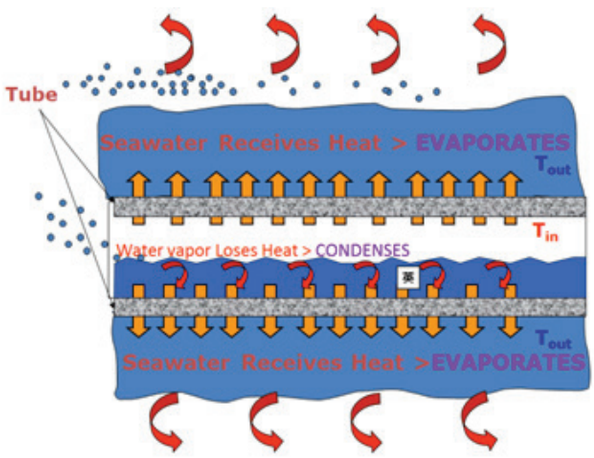

Fig. 2. Condensation (inside of the tube) + Evaporation (outside of the tube).

3.2. Process modeling

The following sections include discussion of the model equations for various components within the system. Common components among various models include constant heat transfer area in each effect, negligible heat losses to the surroundings, and salt free distillate product at steady state operation.

(1) Balance equations for each effect evaporator

The mathematical model for each effect includes the material and energy balances as well as the heat transfer equation. The thermodynamic model was developed based on the mass and energy balance. Total mass and salt balance in effect evaporator i could be described as

$$F_i = D_i + B_i \tag{1}$$

and

$$X_{Fi}F_i = X_{Bi}B_i + X_{Di}D_i \tag{2}$$

In Eqs. (1) and (2), *B*, *D*, and *F* are the flow rate of brine, distillate, and feed respectively. *X* is the salinity, and the subscripts *b*, *f* and *i* represent the brine, feed, and the effect number. After evaporation the salinity of rejected brine could be obtained as

$$X_b = 0.9(457628.5 - 11304.11T_b + 107.5781T_b^2 - 0.3604747T_b^3) \tag{3}$$

This equation is used to calculate the reject brine salinity in each effect as a function of the brine temperature. This equation is obtained by curve fitting of the salinity/temperature relation for the solubility, 90% of the solubility of C_aSO_4. The upper limit on the rejected brine salinity is set at 70,000 ppm.

Total energy balance in effect evaporator *i* could be expressed as

$$D_{i-1}\lambda_{i-1} + d_{i-1}\lambda_{i-1} + d'_{i-1}\lambda'_{i-1} = F_iC_p(T_i - T_f) + D_i\lambda_i \tag{4}$$

In the above equation, *d* is the amount of vapor formed by brine flashing in effect i–1, d'_i is the amount of vapor formed by distillate flashing, λ is the latent, C_p is the specific heat at constant pressure, T_i is the brine temperature after evaporation, and T_f is the feed seawater temperature.

According to the theory of heat transfer the vapor temperature in effect i can be calculated as

$$T_{vi} = T_i - BPE_i \tag{5}$$

where *BPE* is the boiling point elevation and T_v is the vapor temperature. The *BPE* is the boiling point elevation of the liquid, which means that the boiling point of a liquid will be higher when another compound is added. Boiling point elevation effect is affected by many factors during evaporation. There is a nonlinear relationship between the *BPE* and process parameters in each effect evaporator, such as liquid concentration, operating temperature, etc. In engineering *BPE* can be estimated as following [8]

$$\begin{aligned} BPE_i = {} & (8.2543\times10^{-2} + 1.883\times10^{-4}T_{vi} + 4.02\times10^{-6}T_{vi2})X_i \\ & + (-7.625\times10^{-4} + 9.02\times10^{-5}T_{vi} - 5.02\times10^{-7}T_{vi2})X_{i2} \\ & + (1.552\times10^{-3} - 3\times10^{-6}T_{vi} + 3\times10^{-8}T_{vi2})X_{i3} \end{aligned} \tag{6}$$

Similarly the temperature of vapor condensation in effect i can be figured out by

$$T_{ci} = T_i - BPE_i - \Delta T_i \tag{7}$$

In Eq. (7), the condensation temperature, T_{ci}, is lower than the brine temperature, T_i, by the difference in the evaporation temperatures between the effects (ΔT_i). Thus the heat transfer area needed in effect i can be derived based on the energy transfer rate equation.

$$\begin{aligned} & D_{i-1}\lambda_{i-1} + d_{i-1}\lambda_{i-1} + d'_{i-1}\lambda'_{i-1} = F_iC_p(T_i - T_f) + D_i\lambda_i \\ & \quad = A_{1i}U_{1i}(LMTD)_i + A_{2i}U_{2i}(T_{ci} - T_i) \end{aligned} \tag{8}$$

$$\alpha(D_{i-1}\lambda_{i-1} + d_{i-1}\lambda_{i-1} + d'_{i-1}\lambda'_{i-1}) = D_{ii-1i} = A_{2i}U_{2i}(T_{ci} - T_i) \tag{9}$$

$$(LMTD)_i = (T_i - T_f) / \ln((T_{ci} - T_f) / (T_{ci} - T_i)) \tag{10}$$

whereA_{1i} is the heat transfer area for sensible heating of the brine from the feed to the evaporation temperature in each effect and A_{2i} is the heat transfer area for evaporation, U_{1i} and U_{2i} are the corresponding overall heat transfer coefficient, *LMTD* is the logarithmic heat transfer coefficient, and α is the fraction of input heat consumed by vapor formation.

(2) Balance equations for flashing boxes

In a multi-effect plant, the brine and the distillate are fed from effect to effect. Both brine and distillate enter a box in which a lower pressure and a lower boiling point temperature exist. The only possibility to release this surplus energy present under these conditions is through spontaneous vapor production. This process is known as "flashing".

Fig. 3 shows two effects of an evaporation plant with the relevant temperatures and mass flows. If boiling point elevation is neglected, the mass and energy balance leads to two equations for the mass flows produced by brine and distillate flashing.

Amount of vapor formed by the brine flashing inside the effect i can be obtained as

$$d_i = B_{i-1}C_p\frac{T_{i-1} - T'_i}{\lambda_i} \tag{11}$$

with

$$T'_i = T_i + NEA_i \tag{12}$$

In Eq. (11), T_i' is the temperature at which the brine cools down to as it enters the effect i. Also, the latent heat λ_i is calculated at the effect vapor temperature, T_{vi}. The term NEA_i is the non-equilibrium allowance and is calculated from the correlation developed by Miyatake [29]:

$$(NEA)_i = \frac{33.0(T_{i-1} - T_i)^{0.55}}{T_{vi}} \tag{13}$$

Similarly amount of vapor flashed off by the distillate flashing boxes can be calculated according to the formula

$$d'_i = D_{i-1}C_p\frac{T_{ci-1} - T''_i}{\lambda'_i} \tag{14}$$

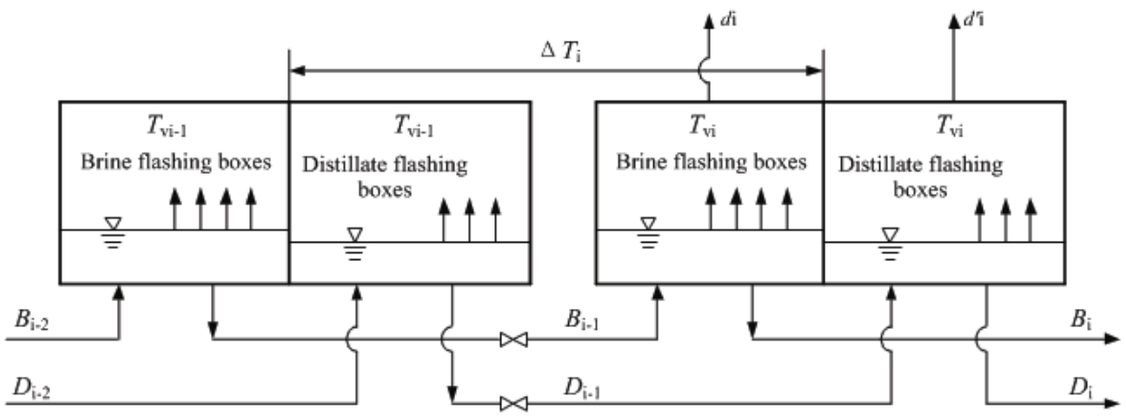

Fig. 3. Illustration of the flashing process in a thermal desalination plant.

with

$$T_i'' = T_{vi} + (NEA)_i \tag{15}$$

where T_i'' is the temperature at which the condensing vapor cools down to as it enters the flashing box.

(3) Balance equations for the condenser

The condenser balance equations include the energy balance and heat transfer rating equation. Energy balance of the condenser was represented as

$$(d_n + d_n' + D_n)\lambda_n = (M_{cw} + M_f)C_p(T_f - T_{cw}) \tag{16}$$

Heat transfer rate of the condenser can be shown as

$$\begin{aligned}(d_n + d_n' + D_n)\lambda_n &= U_c A_c (LMTD)_c \\ (LMTD)_c &= (T_f - T_{cw}) / \ln((T_{vn} - T_{cw}) / (T_{cn} - T_f))\end{aligned} \tag{17}$$

where A_c, U_c, and $(LMTD)_c$ are the heat transfer area, overall heat transfer coefficient, and logarithmic mean temperature difference for condenser respectively.

(4) Model of the steam jet ejector

The calculation model of steam jet ejector is based on the semi-empirical model developed by El-Dessouky [30]. The entrainment ratio is flow rate ratio of the motive steam and the entrained vapor. The entrainment ratio, R_a, is calculated from the following relation

$$R_a = 0.296 \cdot \frac{P_s^{1.19}}{P_{ev}^{1.04}} \cdot \left(\frac{P_m}{P_{ev}}\right)^{0.015} \left(\frac{PCF}{TCF}\right) \tag{18}$$

where P_m, P_s and P_{ev} are the pressures of the motive steam, compressed vapor, and entrained vapor respectively, *PCF* is the motive steam pressure correction factor and *TCF* is the entrained vapor temperature correction factor. The following equation can be used to calculate *PCF* and *TCF*.

$$\begin{aligned}PCF &= 3\times10^{-7} P_m^{\,2} - 0.0009 P_m + 1.6101 \\ TCF &= 2\times10^{-8} T_{ev}^{\,2} - 0.0006 T_{ev} + 1.0047\end{aligned} \tag{19}$$

where the units of P_m and T_{ev} are kPa and °C respectively.

In presence of the steam jet ejector, the thermal load of the down effect i or condenser is lower since part of the vapor formed in the former effect and the associated flashing box is entrained in the steam jet ejector. Therefore, the vapor formed in the entrained vapor effect is defined by

$$M_{ev} + M_u = (d_i + d_i' + D_i) \tag{20}$$

where M_{ev} and M_u are the flow rates of the entrained and un-entrained vapor, respectively.

(5) Performance of MED

For most of the current desalination applications, fuel costs are proportional to the energy input to the system. These costs can either be of a direct nature, when for example fossil fuels are used to drive the system, or of an indirect nature, when for example low pressure steam is extracted from a power plant turbine. Consequently, the rational definition of the efficiency of these systems is related to the specific energy consumption per product water. This is exemplified by the industrial standard GOR for steam driven MED systems, which is the ratio of the distillate production to the steam input,

$$\text{GOR} = M_d / M_m \tag{21}$$

$$M_d = D_1 + D_2 + \ldots + D_{i-1} + D_n \tag{22}$$

where M_m is the mass flow rate of motive steam supplied to the system, and M_d is the mass flow rate of the distillate product. It is worth noting that the contents of distillate production and the steam input is easy to understand combining with the MED-TVC process model shown in Fig. 1. It can be seen from Fig. 1 that the steam input consists of the mass flow rate of motive steam supplied into the system (M_m) only, and does not include the mass flow rate of steam extracted by TVC (M_{ev}). The distillate production (M_d) was formed by the residual fluid of all distillate flashing boxes after flashing. The GOR is a simplification for steam driven systems, where the difference between the latent heat of condensation of the heat source medium and the evaporation energy of the feed can be neglected. It facilitates a quick and effective benchmark for steam driven systems.

The specific heat transfer area is

$$S_A = \frac{\sum_{i=1}^{n} A_i + A_c}{M_d} \tag{23}$$

where A_i is the heat transfer area in effect i and A_c is the condenser heat transfer area.

4. Results and discussion

The mathematical models for the system are interlinked and highly nonlinear for some process parameters such as heat-transfer temperature difference and boiling point elevation of each effect evaporator. Therefore, iterative solution is necessary to calculate the system characteristics. The calculation was specifically implemented using the self-designed software 'MEDGYV2010' which was programmed based on the mass and energy conservation equation, and the nonlinear relationship of heat-transfer temperature difference and boiling point elevation with process parameters. The algorithm embedded in the software of 'MEDGYV2010' is traditional numerical iterative method. The initial conditions adopted in the solving algorithm during numerical calculation were shown in Table 3.

It is worth noting that the overall heat transfer coefficients in the effects are specified and assumed to be constant throughout the paper during the numerical simulation. Evaporation temperature is 70°C. Overall heat transfer coefficient (U_i) is set to 3.49 kW/(m^2·°C). The heat transfer coefficient is reduced by 1% as the temperature decreases by 1°C, and the overall heat transfer coefficient in the condenser (U_c) is set to 1.63 kW/(m^2·°C) [31].

Table 3
The initial conditions using in the solving algorithm during numerical calculation

Parameters	Value
Number of effect evaporators	4–11
Motive steam pressure, MPa	0.8
Heating steam temperature (T_s), °C	60–80
Seawater temperature (T_{cw}), °C	30
The raw seawater TDS, ppm	33000–34000
Salinity of rejected brine (X_b), ppm	66000
Outside (δ_o) and inside (δ_i) diameters of heat transfer tube, mm	19.00 and 17.70
Temperatures difference in the effect evaporations (ΔT_i), °C	2–7
Heat loss coefficient	0.99
Evaporation temperature in the last effect, °C	46.5

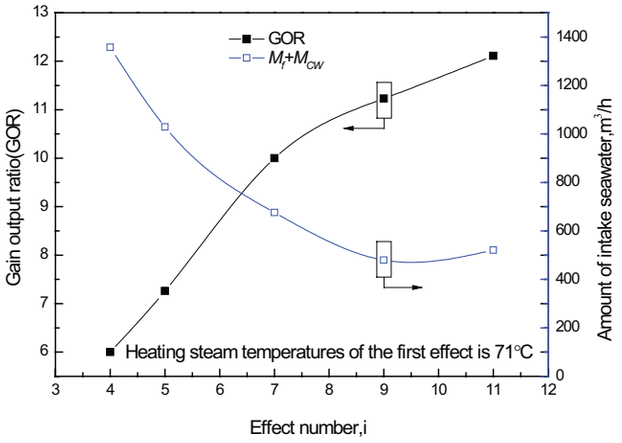

Fig. 4. Changes of GOR and amount of intake seawater with respect to variations in the number of effects.

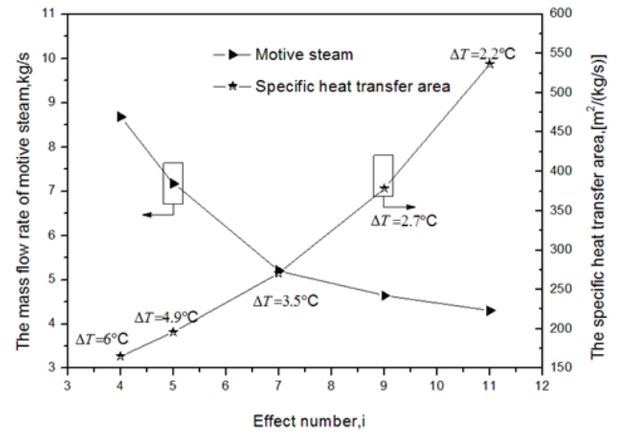

Fig. 5. Changes of the mass flow rate of motive steam and the specific heat transfer area with respect to variations in the number of effects.

The number of effects is one of the most important characteristics of a MED system. Fig. 4 shows the changes in GOR and amount of intake seawater for a constant system capacity when the number of effects is increased. The temperatures of the last effects are the same, but their temperature differences vary. The extraction ports are all located at the last effect. Hence, the operation parameters for the steam jet pumps are the same. Part of the steam in the last effect is drawn by the TVC into the system for recycling. GOR reaches a maximum magnitude of 10 for the seven-effect MED. The feed water flow rate is increased by the model as the number of effects increases to prevent fouling. Heating this amount of feed water to the temperature of the effects reduces the primary steam potential for vapor generation, thereby resulting in lower GOR.

Fig. 4 shows that the GOR continues to grow with increasing number of effects. However, the growth rate is slowly reduced because the temperature difference between effects decreases gradually with an increasing number of effects. Fig. 5 shows that the temperature difference is changed from 6°C to 2.2°C, which indicates that the driving force of evaporation is reduced. The heat transfer efficiency is reduced, although the steam utilizing cycles are increased with the number of effects. The GOR grows fastest from five effects to seven effects and reaches 10 at seven effects. The growth rate of the GOR gradually slows down from nine effects to 11 effects. The GOR will reach to 12.11 when adopting 11 effect evaporators.

The total amount of intake seawater usually includes the cooling seawater and feed water. The amount of required cooling seawater is directly proportional to the condenser inlet steam flow rate, which is equal to the amount of steam produced in the last effect minus the amount sucked out by the TVC. Fig. 4 shows that the total amount of intake seawater first decreases and then increases with increasing number of effects. This phenomenon is due to the decrease in the amount of steam entering the condenser with the increase in the number of effects. The amount of cooling water for condensation of the steam is reduced as the steam to be condensed is reduced when the latent heat of vaporization and the temperature of the seawater are constant. Fig. 4 shows that the total amount of intake seawater at seven effects is 676 m^3/h, which is half the amount at four effects. Thus, the energy consumption of the pump is largely reduced. Moreover, the electricity consumption of each ton of water is reduced by 0.3 kWh, because the amount of steam to be condensed at seven effects is 4.1 kg/s, which is 41% lower than at four effects.

However, the amount of steam entering the condenser at nine effects is 2.0 kg/s, and the amount of cooling water needed is 311 m^3/h, which is lower than the amount of feed water (M_f), which is 479.2 m^3/h. The amount of steam entering the condenser at 11 effects is 0.98 kg/s, and the amount of cooling water needed is 143 m^3/h, which is lower than the amount of feed water, which is 520.8 m^3/h. Fig. 6 shows that the total amount of intake seawater is the sum of the amount of feed water and the amount of cooling water ($M_f + M_{CW}$) when the number of effect is lower than nine, and M_f when effects are larger than nine. The feed water flow

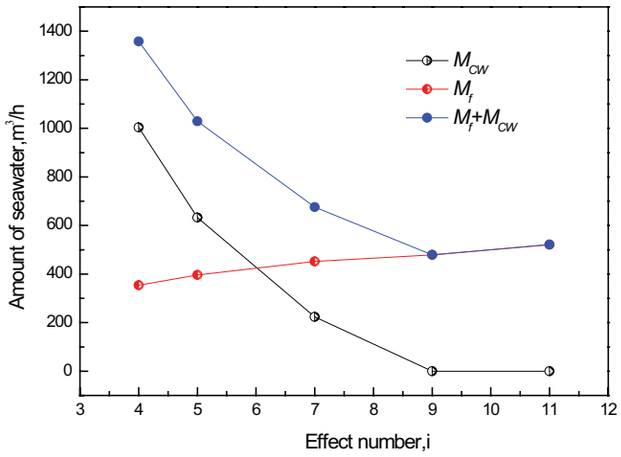

Fig. 6. Changes of the amount of seawater with respect to variations in the number of effects.

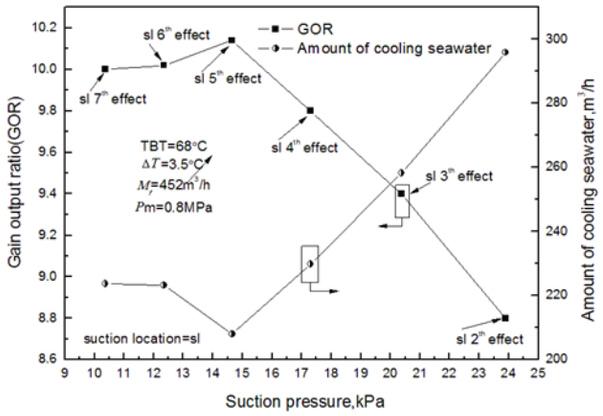

Fig. 7. Changes of GOR and amount of cooling seawater with respect to variations in the suction pressure.

rate M_f is increased by the model as the number of effects increases to ensure sprinkle density and prevent fouling. The amount of the total intake seawater at a certain number of effects is determined by the quantity of water rather than the amount of the cooling water to condense the steam at the last effect to ensure the spray density (generally 240 L/(m·h) ~300 L/(m·h)) in the evaporator. Sprinkle density is the spraying volume of per meter length on the surface of one heat exchange tube in one hour. This parameter can be calculated as follows:

$$\text{Sprinkle density} = F_i \times 1000/L \times N \ (\text{l/h/m}) \quad (24)$$

where F_i is the flow rate of fed seawater of effect i, L is the length of heat exchange tube, and N is the total number of pipes on the same layer.

Fig. 5 illustrates the variations in the specific heat transfer area of effects and the mass flow rate of motive steam when the number of effects is changed. The increase in the specific heat transfer area of effects is due to the increase in the number of effects when the production is constant. This result is in agreement with the charts presented by El-Dessouky [9]. Assuming that the seawater temperature is 30°C, the temperature difference at the same end (TBT) is 68°C, and the evaporation temperature in the last effect is 46.5°C, the seven-effect model has a lower specific heat transfer area and less motive steam than the other models. Specific heat transfer area is the ratio of the heat transfer surface of the effects to the production flow rate.

Approximately 3°C is the commonly adopted temperature difference for conventional systems. However, temperature drops of as low as 1.5–2.5°C can be achieved for commercial applications with a cost-optimized material selection and heat exchanger design. Temperature difference is restricted to the range of 3–4°C based on typical operating conditions. This limited range is critical to obtain a high heat transfer coefficient and a steady operating condition.

Figs. 4–6 show that the seven-effect MED process has many advantages, namely, higher GOR, lower amount of intake seawater, lower specific heat transfer area, and less motive steam, compared with the other models. The TBT is the highest temperature the seawater can reach in the system, which is typically the temperature of the brine in the first effect. The TBT is imposed by either the heat source temperature or material limitations to avoid excessive scaling and corrosion. This maximum temperature for seawater applications is commonly set to between 62 and 75°C depending on the local seawater composition. In this paper, a set of multi-effect, flash, and TVC technology as one of the overall process scheme (MED-TVC) is formed. The process scheme uses seven effects of MED with each effect using the same structure. The key design parameters were selected based on the pilot test and laboratory findings [23]. The heating steam temperature of the first effect is 71°C. The temperature difference between each effect is 3.5°C. The steam jet ejector is set up for steam recycling and pumping part of the secondary steam in the seventh effect to the first effect.

Fig. 7 shows the GOR and amount of cooling seawater as a function of the suction pressure of the thermo compressor. Moving the suction location of the thermo compressor to the middle effects increases the entrainment ratio of the thermo compressor. This phenomenon is due to the decrease in the compression ratio. Increasing the entrainment ratio will reduce the energy consumption of the system. However, that part of vapor is recycled in the system by moving the suction location. Therefore, shifting the suction location of the thermo compressor in the effects with higher pressure will increase energy consumption. At the same time, the amount of cooling seawater is increased, which will increase the energy consumption of the cooling seawater pump. The best suction pressure is always an intermediate pressure, that is, between 10.4 and 14.6 kPa, to achieve the maximum GOR of the system regardless of the amount of the motive steam pressure. This is consistent with what the published articles recommends [23,32]. In the design, the diameter of the evaporator cylinder is generally kept constant such that the length of the heat transfer tube of the effects after the extraction port is reduced, and the structure of the evaporator differs from the effects ahead.

If the extraction port is set in the condenser (the secondary steam is extracted from the seventh effect), then the size and structure of the effects ahead are basically the same. Thus, the processing accuracy will be improved, costs will be reduced, and higher GOR is obtained. Therefore, in the process discussed in this article, the extraction port is set on the condenser, and the secondary steam of the seventh effect is extracted.

Fig. 8 includes profiles for the distillate flow rates generated in the flash box and in the effect by evaporation and flashing. Results indicate that the major portion of the total product is formed by evaporation within the effect. In addition, evaporation rates are higher at the first effect and decrease in subsequent effects, where the latent heat of vaporization is smaller at higher temperatures. An upward trend in production is observed at effects greater than five. This production growth in the last effect at a higher number of effects is due to the significant steam production by brine and distillate flashing. The amount of the flash steam is gradually increased as the distillate is accumulated gradually from the first effect to the last effect. The amount of flash steam is gradually increased, because the amount of brine increases as the grouping of the first three effects. However, the amount of the brine is not increase dafter the fourth effect. The amount of the flash steam is gradually decreased as the flash efficiency is reduced by the heat loss. Brine flashing, which accounts for 3.9% of the total water production, has a larger contribution than distillate flashing. Brine and distillate flashing accounts for 6.0% of the total water production, which indicate the significant effect of such heat recovery method.

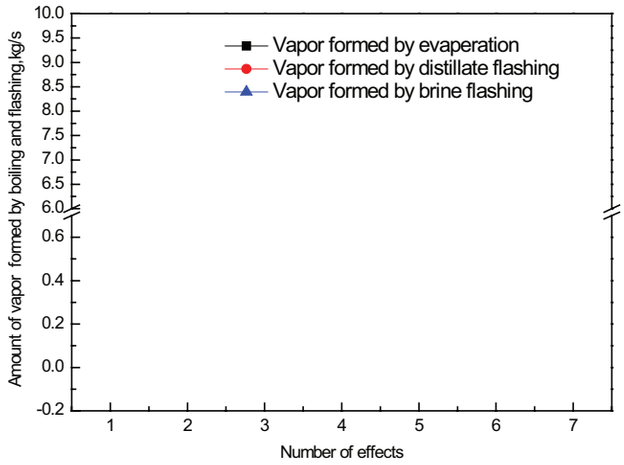

Fig. 8. Changes of amount of vapor formed by boiling and flashing with respect to variations in the number of effects.

Through the above analysis the main process design parameters could be obtained based on the above-mentioned design model, which is shown in Tables 4 and 5. As the core component of TVC, the steam jet vacuum pump plays an important role in the performance of the desalination system. The main performance indicator of the steam jet vacuum pump is injection coefficient (R_a). The simulation result of this indicator was calculated according to the compression ratio and expansion ratio during operation, and shown in Table 5.

5. System structure and materials

The desalination plant consists of seven evaporators and a condenser in series, which are connected by welding. A flow schematic containing process parameters such as steam flow, temperature and pressures at key point under the design condition is illustrated in Fig. 9. Total length of the plant is 56 m, height at the center line is 7.8 m, and total weight is 331 t (as shown in Fig. 10).

The evaporators and condenser are cylindrical (4.5 min diameter and 5–6.8 m long) and weigh 36–48 t. The evaporators are bolted to the supports, which are welded by the columns and connecting rods. A total of 34 columns made from steel tubes (5.3 m high, 377 mm outside diameter and 9

Table 5
Simulation results of flow rate in the MED system

Parameter	Value
$T_{cw,}$ °C	30
$M_{cw,}$ m^3/d	4400
R_a	0.9
$M_{f'}$ m^3/d	10850
$M_{b'}$ m^3/d	6350
$M_{d'}$ m^3/d	4500

Table 4
Simulated calculation results of process parameters

Effect/ condenser	1	2	3	4	5	6	7	Condenser
$T_{v'}$ °C	67.5	64	60.5	57	53.5	50	46.5	
$T_{i'}$ °C	68.2	64.7	61.2	57.5	54.0	50.5	46.9	43.4
$T_{f'}$ °C	54.02	54.02	54.02	43.00	43.00	43.00	43.00	30.00
BPE	0.70	0.68	0.65	0.46	0.45	0.44	0.44	0.00
$X_{cw,}$ ppm	44.68	44.68	44.68	34.00	34.00	34.00	34.00	34.00
$X_{bn,}$ ppm	62.18	60.36	59.58	44.56	44.38	44.58	45.21	34.00
Product water of each effect D_i, m^3/h	35	32	30	29	28	27	28	14

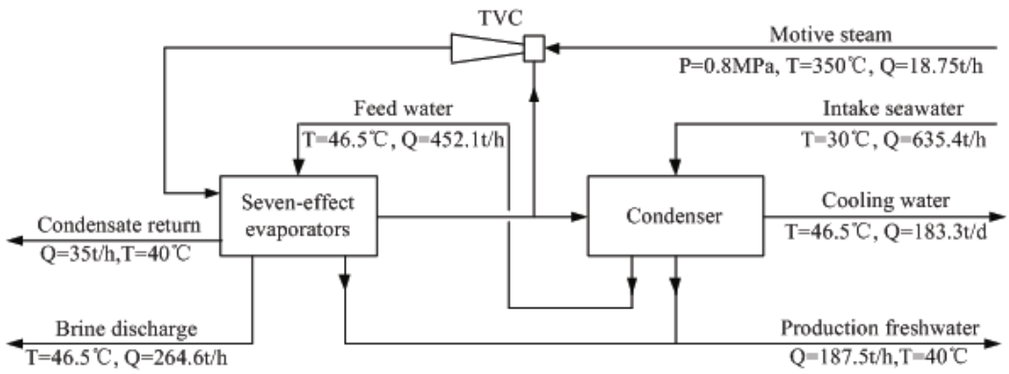

Fig. 9. The flow schematic containing process parameters at key point under the design condition.

Fig. 10. Indonesia 2 × 4500 m^3/d MED plant.

mm thick) are installed. Some auxiliary equipment, namely, one main steam compression injector, one three-stage vacuum pump, one start vacuum pump, two heat exchangers, and thirteen flashing boxes, are also equipped according to the process.

Metals and FRP are the two main materials for all pipelines. Steam pipes are metal pipelines made from stainless steel. Seawater and fresh water pipes are FRP pipelines. All piping systems are low-pressure pipelines. The pressure of the steam inlet pipeline varies from 0.8 MPa to 1.2 MPa, and the rest are less than 0.2 MPa. The main pipelines have negative pressure from 0.02 MPa to 0.07 MPa.

Table 6 shows the plant configurations and materials used in manufacturing the plant.

6. Performance of system operation

The measuring instruments including pressure gauge, temperature gauge, flowmeter, fluid level meter online conductivity and pH were used to monitor the operating state of the desalination device. In our operational test, the orifice plate flowmeter is used to measure steam flow rate with temperature and pressure compensation to ensure a measurement error of less than ±0.1%. Product water quality was monitored by using an online conductivity meter and a pH meter installed on the product pump outlet. The host computer records and stores all in situ operation data automatically.

Motive steam fluctuates slightly during operation. However, the operating conditions are constant, as follows: pressure, 0.8 MPa; temperature, 350°C; salinity, from 33000 mg/L to 34000 mg/L; and average seawater temperature, 30.2°C. A single unit capacity of produced water is 196.4 t/h (4712.4 t/d), product water conductivity is 15.9 μs/cm (7.98 mg/L), and condensate water conductivity is 3.43 μs/cm. Consumption of motive steam is approximately 18.98 t/h. GOR of the device is 10.3, which is higher than the design value of 10. The system operation performance parameters are given in Table 7 and compared with the design value that was obtained by solving the established model with the help of the iterative algorithm.

Table 6
Structure size and configuration

Serial number	Description of the structure/configuration	Type	Dimensions/ model	Material and brand	Remarks
1	Shells of the evaporator	Horizontal	ϕ4.5 m, *l* = 6 m	SS 316L	/
2	Pipe bundle in evaporator	Smooth tube	ϕ19, *l* = 4 m	The first three rows is titanium tube, others is Aluminium brass tube	Titanium tube to prevent erosion
3	Tube plate	Block assembly	Thickness δ = 20	SS316L	/
4	Vapor compressor(TVC)	Thermo-compression	DN250/1200	SS 304	Nozzle of the injection is SS316L
5	Shell of the condenser	Falling film	ϕ4.5 m, *l* = 4m	SS316L	/
6	Pipe bundle in condenser	Smooth tube	ϕ19, *l* =2 m	Titanium tube	/
7	Mist eliminator	Louver type	/	SS316L	/
8	Exhaust system and vacuum pump	Three-stage steam jet pump	DN50/450	/	The operational pressure of the steam: 0.26~1.4MPa.a
9	Heat exchanger	Shell-and-Tube type	69.8 m^2/72 m^2	Titanium	Condensate exchanger/ Product exchanger
10	Pipes	/	/	Stainless steel or fiber glass steel	/
11	Valves	Butterfly valve, gate valve, shut-off valve, etc	/	SS316 or rubber lining	/

Table 7
System operation performance parameters when the motive steam pressure is 0.8 MPa

Serial number	Items of parameters	Operation value	Model value	Remarks
1	Production capacity, m^3/d	4712.4	4500	
2	GOR	10.3	10.0	
3	Steam consumption, t/h	18.98	18.75	Only heating steam consumption is included
4	Product water quality, ppm	7.98	10	
5	The first effect vapor temperature, °C	67.36	67.50	
6	Condensate flow, t/h	35.1	35.0	
7	Condensate temperature, °C	36.12	40	
8	Flow of brine discharge, t/h	261.0	264.6	
9	Top brine temperature (TBT), °C	67.7	68.3	
10	Amount of intake seawater, t/h	626.2	635.4	
11	Flow of discharge cooling seawater, t/h	179.7	183.3	Seawater temperature is 30°C

Table 7 shows that the operation value of the system GOR is higher than the design value, which is probably caused by two reasons. First, the heat transfer coefficient varies according to the variation in the evaporation temperature. Data are derived from the experimental results obtained on the multifunction heat transfer platform and engineering experience. Second, the processing costs of the evaporator are reduced, and the precision of the tube plate evaporator is improved. Moreover, the heat transfer tubes are arranged in the same way, as much as possible, as that of a certain effect. Thus, the actual number of installed heat transfer tubes is slightly greater than the simulation number, and the fresh water ratio increases.

Table 7 shows that the error between the operation performance parameters and the model value is less than 5%. The operation performance parameters are significantly better than the model value. This characteristic indicates that the simulation model established in this article is accu-

rate and can provide a reliable tool for designing future desalination plants.

7. Conclusions

(1) This work introduces the overall design, process scheme selection,operation parameters and performance comparison analysis of a seven-effect 2 × 4500 m^3/d low-temperature multi-effect desalination plant located in Indramayu, Indonesia. The technical framework of counter current flow, grouped feeding method and flashing of concentrated brine and distilled water are adopted based on the quality of raw seawater and conditions of steam source, worksite and design requirements. Simultaneously, a TVC device was installed to improve the overall efficiency of the desalination system. On this basis the thermodynamic calculation model of the total desalination system was formulated. The injection coefficient was introduced to manifest the performance of TVC in the simulated model.

(2) On the basis of the model, the influences of the number of effect evaporator on the system GOR, amount of intake seawater, mass flow rate of motive steam and the specific heat transfer area were investigated emphatically. The number of effect evaporators selected in the large scale seawater desalination equipment should take into consideration the factors of the equipment investment and operational performance. The case study of 2 × 4500 m^3/d practical desalination project could provide a good guidance in the determination method of key technical parameters (number of effect evaporators) for large scale MED-TVC device. Besides simulation results showed that the best suction pressure of TVC is always at an intermediate value between 10.4 and 14.6 kPa to achieve the maximum GOR for the seven effects system regardless of the amount of the motive steam pressure. Simulation results show that heat recovery method by brine and distillate flashing has a significant effect. Brine flashing, which accounts for 3.9% of the total water production, has a larger contribution compared with distillate flashing. Brine and distillate flashing account for 6.0% of the total water production.

(3) n accordance with the simulation results, Indonesia Indramayu 2 × 4500 m^3/d MED desalination device with seven effect evaporators and TVC is designed and built. The plant has a total length of 56 m. The evaporator has an inner diameter of 4500 mm, and the shell cylinder material is SS316L. The height of the center line is 7.8 m, and the total weight is 331 t. The tested data indicated that the error between the actual operation performance parameters and the simulated model value is less than 5%. The operation performance parameters are significantly better than the model value. The operating results illustrate that the simulation model established in this article is accurate and can provide a reliable tool for designing future desalination system especially the design and construction of desalination facility in the dual-purpose power plant.

Acknowledgements

The authors are grateful for the support of natural science foundation of Tianjin (NO.16JCYBJC19400). This paper is also supported by Projects in the National Science & Technology Pillar Program during the Twelfth Five-year Plan Period No. 2014BAB04B02 and No. 2015BAB08B01.

Symbols

A_{1i}	—	Heat transfer area for sensible heating of the brine from the feed to the evaporation temperature in each effect, m^2
A_{2i}	—	Heat transfer area for evaporation, m^2
A_c	—	Heat transfer area for condenser, m^2
B	—	Flow rates of brine, m^3/h
C_p	—	Specific heat at constant pressure, kJ/(kg·°C)
D	—	Flow rates of distillate, m^3/h
d_i'	—	Amount of vapor formed by distillate flashing, m^3/h
F	—	Flow rates of feed, m^3/h
M	—	Flow rate of the vapor for TVC, m^3/h
n	—	Number of effect evaporators
P	—	Pressure, MPa
P_m	—	Pressure of motive steam for TVC, MPa
P_s	—	Pressures of compressed vapor for TVC, MPa
P_{ev}	—	Pressure of entrained vapor for TVC, MPa
R_a	—	Injection coefficient of steam injection pump
T	—	temperature, °C
U_{1i}, U_{2i}	—	Corresponding overall heat transfer coefficient, kW/(m^2·°C)
U_c	—	Overall heat transfer coefficient for condenser, kW/(m^2·°C)
X	—	Salinity, mg/L
α	—	Fraction of input heat consumed by vapor formation
λ	—	Latent heat, kJ/kg
ΔT	—	Temperature difference between the effect evaporator, °C

Subscripts

B	—	Brine
f	—	Feed
i	—	Effect number
c	—	Condenser
sw	—	Seawater
s	—	Motive steam
v	—	Vapor

References

[1] Global Water Intelligence. IDA Desalination Yearbook 2015–2016, Media Analytics Ltd., Oxford, September 1st, 2015, pp.1–10.

[2] K.C. Ng, K. Thu, S.J. Oh, L. Ang, M.W. Shahzad, A.B. Ismail, Recent developments in thermally-driven seawater desalination: Energy efficiency improvement by hybridization of the MED and AD cycles, Desalination, 356 (2015) 255–270.
[3] M.W. Shahzad, K.C. Ng, On the road to water sustainability in the Gulf, http://www.natureasia.com/en/nmiddleeast/article/10.1038/nmiddleeast.2016.50.
[4] Y. Ghalavanda, M.S. Hatamipoura, A. Rahimia, A review on energy consumption of desalination processes, Desal. Water. Treat., 54 (2015) 1526–1541.
[5] C.H. Qi, H.J. Feng, H.Q. Lv, C. Miao, Numerical and experimental research on the heat transfer of seawater desalination with liquid film outside elliptical tube, Int. J. Heat Mass Tran., 93 (2016) 207–216.
[6] I.J. Esfahani, A. Ataei, K.S. Vidya, T. Oh, J.H. Park, C.K. Yoo,-Modeling and genetic algorithm-based multi-objective optimization of the MED-TVC desalination system, Desalination, 292 (2012) 87–104.
[7] M.A. Sharaf, A.S. Nafey, L. Garcia-Rodriguez, Thermo-economic analysis of solarthermal power cycles assisted MED-VC (multi effect distillation-vapor compression) desalination processes, Energy, 36 (2011) 2753–2764.
[8] A.O. Bin Amer, Development and optimization of ME-TVC desalination system, Desalination, 249 (2009) 1315–1331.
[9] H. El-Dessouky, H.M. Ettouney, F. Mandani, Performance of parallel feed multi effect evaporation system for seawater desalination, Appl. Therm. Eng., 20 (2000)1679–1706.
[10] D.F. Zhao, J.L. Xue, S. Li, H. Sun, Q.D. Zhang, Theoretical analyses thermal and economical aspects of multi-effect distillation desalination dealing with high salinity wastewater, Desalination, 273 (2011) 292–298.
[11] K.C. Ng, K. Thu, M.W. Shahzada, W. Chun, Progress of adsorption cycle and its hybrids with conventional multi-effect desalination processes, IDA J. Water Reuse Desal., 6 (2014) 44–56.
[12] H.A. Ahmed, I.M. Ismail, W.F. Saleh, M. Ahmed, Experimental investigation of humidification-dehumidification desalination system with corrugated packing in the humidifier, Desalination, 410 (2017) 19–29.
[13] V.G. Gude, Desalination and sustainability-An appraisal and current perspective, Water Res., 89 (2016) 87–106.
[14] M.W. Shahzad, K. Thu, K.C. Ng, W.G. Chun, Recent development in thermally activated desalination methods: achieving an energy efficiency less than 2.5 kWh_{elec}/m^3, Desal. Water Treat., 57/16 (2016) 7396–7405.
[15] M.W. Shahzad, K. Thu, Y.D. Kim, K.C. Ng, An experimental investigation on MEDAD hybrid desalination cycle, Appl. Energ., 148 (2015) 273–281.
[16] M.W. Shahzad, K.C. Ng, K. Thu. Future sustainable desalination using waste heat: kudos to thermodynamic synergy, Environ. Sci.: Water Res. Technol., 2 (2016) 206–212.
[17] F.N. Alasfour, M.A. Darwish, A.O. Bin Amer, Thermal analysis of ME-TVC + MEEdesalination systems, Desalination, 174 (2005) 39–61.
[18] H. Ettouney, Visual basic computer package for thermal and membrane desalination processes, Desalination, 165 (2004) 393–408.
[19] A.S. Hanafi, G.M. Mostafa, A. Waheed, A. Fathy, 1-D Mathematical modeling and CFD investigation on supersonic steam ejector in MED-TVC, Energy Procedia, 75 (2015) 3239–3252.
[20] N.H. Aly, M.A. Marwan, Dynamic response of multi-effect evaporators, Desalination, 114 (1997) 189–196.
[21] D. Kumar, V. Kumar, V. Singh, Modeling and dynamic simulation of mixed feed multi-effect evaporators in paper industry, Appl. Math. Model, 37 (2013) 384–397.
[22] A.DL. Calle, J. Bonilla, Dynamic modeling and performance of the first cell of a multi-effect distillation plant, Appl. Therm. Eng., 70 (2014) 410–420.
[23] C.H. Qi, H.J. Feng, Q.C. Lv, Y.L. Xing, N. Li, Performance study of a pilot-scale low-temperature multi-effect desalination plant, Appl. Energ., 135 (2014) 415–422.
[24] S. Mussati, P. Aguirre, N. Scenna, Dual-purpose desalination plants Part II: Optimal configuration, Desalination, 153 (2003) 185–189.
[25] M.W. Shahzad, K.C. Ng, K. Thu, B.B. Saha, W.G. Chun, Multi effect desalination and adsorption desalination (MEDAD): A hybrid desalination method, Appl. Therm. Eng., 72 (2014) 289–297.
[26] J. Gebel, S. Yüce, An engineer's guide to desalination, VGB PowerTech Service GmbH, Essen, Germany, 2008.
[27] H.T. El-Dessouky, H.M. Ettouney, Fundamentals of Salt Water Desalination, Elsevier, New York, 2002.
[28] K. Bourouni, R. Martin, Heat transfer and evaporation in geothermal desalination units, Appl. Energ., 64 (1999) 129–147.
[29] O. Miyatake, K. Murakami, Y. Kawata, T. Fujii, Fundamental experiments with flash evaporation, Heat Transfer-Jpn. Res., 2 (1973) 89–100.
[30] El-Dessouky, Modeling and simulation of thermal vapor compression desalination plant, Symposiumon Desalination of Seawater with Nuclear Energy. Taejon, Korea, May, 1997, 26–30.
[31] C.H. Qi, Y. Li, Experimental study on heat-transfer coefficients of horizontal tube falling-film evaporation equipment, Chem. Industry Eng., 5 (2011) 1–5.
[32] R. Kouhikamali, M. Sanaei, M. Mehdizadeh, Process investigation of different locations of thermo-compressor suction in MED-TVC plants, Desalination, 280 (2011) 134–138.